ECOLE POLYTECHNIQUE

CENTRE DE MATHÉMATIQUES APPLIQUÉES
UMR CNRS 7641

91128 PALAISEAU CEDEX (FRANCE). Tél: 01 69 33 41 50. Fax: 01 69 33 30 11
http://www.cmap.polytechnique.fr/

Report on the numerical approximation of parabolic problems with highly oscillating coefficients using a multiscale finite element method

Robert BRIZZI and Grégoire ALLAIRE

R.I. 598 *May 2006*

Report on the numerical approximation of parabolic problems with highly oscillating coefficients using a multiscale finite element method

Robert BRIZZI and Grégoire ALLAIRE
CMAP, UMR-CNRS 7641, Ecole Polytechnique
91128 Palaiseau Cedex (France)

May 29, 2006

Abstract

In a previous paper [1], a multiscale finite element method was introduced for performing numerical homogenization in the case of scalar elliptic boundary value problems with highly oscillating coefficients. The present report shows that the use of such a method is also possible for numerical approximation of the solution of parabolic equations which model many problems in science and engineering such that chemical diffusion of radionucleides in highly heterogeous media.

1 Introduction

The aim of the GdR [1] MOMAS of the CNRS is to develop numerical methods to simulate radioactive waste management problems in deep geological formation. Thus, the knowledges of the mean field solution but also of the local fluctuations in a highly heterogeneous problem are very important in many applications. Diffusion in porous media is an example. The major difficulty for numerical simulation is to take into account the spatial variability of the parameters used to characterize the relevant physical properties of the medium : classical finite element methods (or any other methods) give good approximation only if the mesh size is smaller than the finest scale and this leads to prohibitively large amount of computer memory and CPU time. Thus, a direct simulation of such problems exceeds the existing computer resources. In a previous work, a new multiscale finite element was introduced [1] to overcome these difficulties for scalar elliptic boundary value problems. This method was developped in the spirit of Hou and Wu's ([8], [9]). In

[1] GdR : in french *Groupement de Recherche*

this report, we extend this method to the numerical approximation of the solution of a parabolic problem.
In the following, the notation $\varepsilon > 0$ stands for some small scale. Let Ω be a bounded open set of $\mathbb{R}^n$ and let Γ^0 and Γ^1 be a partition of the boundary $\partial\Omega$ of Ω. We denotes by ν denoting the exterior unit normal to $\partial\Omega$.
Let $T > 0$ be a given positive number. We set

$$\Omega_T \;=\; \Omega\times]0,T[\;,\;\; \Gamma_T^i \;=\; \Gamma^i\times]0,T[\quad (i=0,1).$$

Let $f \in L^2\left(0,T;H^{-1}(\Omega)\right)$ and let $\Phi \in C^1([0,T])$ be the function with compact support inside the interval $]0,T[$ such that $\Phi(0) = 0$. Let $u_0 \in L^2(\Omega)$. Our model problem is to find a function u^ε satisfying

$$\left\{\begin{array}{rcll} \rho^\varepsilon \dfrac{\partial u^\varepsilon}{\partial t} - \mathrm{div}\{A^\varepsilon \,\mathrm{grad}\, u^\varepsilon\} & = & f & \text{in } \Omega_T \\ u^\varepsilon & = & 0 & \text{on } \Gamma_T^0 \\ \dfrac{\partial u^\varepsilon}{\partial \nu_{A^\varepsilon}} & = & \Phi(t) & \text{on } \Gamma_T^1 \end{array}\right. \tag{1}$$

where the notation $\dfrac{\partial u^\varepsilon}{\partial \nu_{A^\varepsilon}}$ stands for $A^\varepsilon \mathrm{grad}\, u^\varepsilon \,.\, \nu$.
Furthermore, the solution u^ε satisfies the initial condition

$$u^\varepsilon(0,x) \;=\; u_0. \tag{2}$$

In the present work, all the characteristic properties of the medium are given data which are assumed to be independant on t. We assume that $\rho^\varepsilon \in L^\infty(\Omega)$ and that there exists two positive constants λ_1 and λ_2 such that $0 < \lambda_1 < \rho^\varepsilon < \lambda_2$ a.e in Ω.
The matrix $A^\varepsilon = (a_{ij}^\varepsilon)_{i,j=1}^n$ is non-necessarily symmetric and all the coefficients belong to $L^\infty(\Omega)$. We assume that A^ε is uniformly bounded and coercive.
This report has been organized into two parts. The first one (sections 2 and 3) concerns the straightforward extension of our multiscale approach developped in [1]. The second part (section 4) deals with numerical experiments of the algorithm previously described to highly heteregeneous unstationary problems with applications to the storage of nuclear waste.

2 Homogenization theory and approximate variational formulation

2.1 H-convergence and oscillating test functions

The variational formulation of (1) is classical. Let V be the functional space $V \;=\; \left\{\, v \in H^1(\Omega)\,;\; v \;=\; 0 \,\text{on}\, \Gamma^0 \right\}$ and denote $a^\varepsilon(.,.)$ the continue and co-

ercive bilinear form over $H^1(\Omega)$ associated to the operator A^ε :

$$a^\varepsilon(u,v) \;=\; \int_\Omega A^\varepsilon \mathrm{grad}\, u \cdot \mathrm{grad}\, v \, dx.$$

Then u^ε is the unique function in $L^2(0,T;V) \cap C^0\left([0,T];L^2(\Omega)\right)$ which satisfies, for all v in V,

$$\frac{d}{dt}\left(\rho^\varepsilon(x)\, u^\varepsilon(t), v\right)_{L^2(\Omega)} \;+\; a^\varepsilon(u^\varepsilon(t), v) \;=\; (f,v)_{L^2(\Omega)} \;+\; \int_{\Gamma^1} \Phi(t)\, v d\sigma \qquad (3)$$

and the initial condition

$$u^\varepsilon(0) = u_0. \qquad (4)$$

We know that, up to a subsequence, the sequence of matrices $A^\varepsilon \in L^\infty(\Omega; \mathcal{M}_{\alpha,\beta})$ H-converges, when ε tends to zero, to a homogenized matrix $A^* \in L^\infty(\Omega; \mathcal{M}_{\alpha,\beta})$ where, for given positive constants $\alpha > 0$ and $\beta > 0$, $\mathcal{M}_{\alpha,\beta}$ is the subspace of square real matrices of order n (denoted by $\mathcal{M}_n$) which are coercive as well as their inverses

$$\mathcal{M}_{\alpha,\beta} \;=\; \left\{ M \in \mathcal{M}_n \,;\; M\xi.\xi \geq \alpha|\xi|^2 \,,\; M^{-1}\xi.\xi \geq \beta|\xi|^2 \,,\; \forall \xi \in \mathbb{R}^n \right\}.$$

(for details on H-convergence theory see e.g. [10], [2]).
The sequence of solutions u^ε of (1) satisfies

$$\begin{array}{rcll} u^\varepsilon & \rightharpoonup & u^* \text{ weakly in } L^2(0,T;V) & (\varepsilon \to 0), \\ A^\varepsilon \mathrm{grad}\, u^\varepsilon & \rightharpoonup & A^* \mathrm{grad}\, u^* \text{ weakly in } L^2\left(0,T;L^2(\Omega)^n\right) & (\varepsilon \to 0), \end{array}$$

where $u^* \in L^2(0,T;V) \cap C^0\left([0,T];L^2(\Omega)\right)$ is the solution of the homogenized problem

$$\left\{ \begin{array}{rcll} \rho^* \dfrac{\partial u^*}{\partial t} - \mathrm{div}\{A^* \,\mathrm{grad}\, u^*\} & = & f & \text{in } \Omega_T \\ u^* & = & 0 & \text{on } \Gamma_T^0 \\ \dfrac{\partial u^*}{\partial \nu_{A^*}} & = & \Phi(t) & \text{on } \Gamma_T^1 \end{array} \right. \qquad (5)$$

satisfying the initial condition $u^*(0) \;=\; u_0$. Further, we also know that $u^\varepsilon \;\to\; u^*$ strongly in $L^2\left(0,T;L^2(\Omega)\right)$.
The existence of the so-called *oscillating test functions* is the key point of the sequential compactness property which defines the H-limit of the sequence $(A^\varepsilon)_{\varepsilon>0}$. These ones are neither explicit (they depend on A^*) nor unique (they are unique up to the addition of a sequence converging strongly to

zero in $H^1(\Omega)$). As in [1], we define them as the solutions of the following abstract boundary value problems ($j = 1, ..., n$)

$$\left\{ \begin{array}{rcll} -\mathrm{div}\{A^\varepsilon \ \mathrm{grad}\ \widehat{w}_j^\varepsilon\} & = & -\mathrm{div}\{A^*\, e_j\} & \text{in } \Omega \\ \\ \widehat{w}_j^\varepsilon & = & x_j & \text{on } \partial\Omega. \end{array} \right. \tag{6}$$

where $(e_j)_{j=1,n}$ denotes the canonical basis of $\mathbb{R}^n$.

2.2 An approximate variational formulation

As in the elliptic case, we can immediatly deduce from corrector results (see [1] and [7]) that, if the homogenized solution is smoother, say $u^* \in L^2\left(0,T;W^{2,\infty}(\Omega)\right)$, then

$$u^\varepsilon = u^* + \sum_{i=1}^{n} (\widehat{w}_i^\varepsilon(x) - x_i)\, \frac{\partial u^*}{\partial x_i} \ + \ r'_\varepsilon \tag{7}$$

where the remainder r'_ε converges strongly to zero in $L^2\left(0,T;H^1(\Omega)\right)$. The same remark on the corrector result developped in [1] is available : the right-hand side of formula (7) looks like the first order Taylor expansion of u^* at the point $\widehat{w}^\varepsilon(x) = (\widehat{w}_1^\varepsilon(x), ..., \widehat{w}_n^\varepsilon(x))$ and indicates that $u^\varepsilon(x,t)$ may well be approximated by $u^*(t) \circ \widehat{w}^\varepsilon(x)$. Thus, assuming $u^* \in L^2\left(0,T;W^{2,\infty}(\Omega)\right)$, the representation of the solution u^ε takes the form :

$$u^\varepsilon(x,t) \ = \ u^*\left(\widehat{w}^\varepsilon(x),t\right) \ + \ \widehat{r}^\varepsilon(t,x) \tag{8}$$

where $\widehat{w}_j^\varepsilon$ denotes the family of oscillating test functions defined in (6) and $\widehat{r}^\varepsilon$ the remainder term which converges strongly to zero in $L^2\left(0,T;V\right)$. Following [1] and denoting $\widehat{W}^\varepsilon(x,t) = (\widehat{w}_1^\varepsilon(x), \ldots, \widehat{w}_n^\varepsilon(x), t)$, we can see that the approximation of *the principal part of the solution* u^ε, i.e. $u^* \circ \widehat{W}^\varepsilon$, may serve as a substitute for the approximation of the solution of problem (1). The representation formula (8) for u_ε suggests an approximation of the variational formulation (3)-(4). Indeed, it is equivalent to

$$\begin{array}{rcl} \dfrac{d}{dt}\left(\rho^\varepsilon(x)\, u^* \circ \widehat{W}^\varepsilon, v\right)_{L^2(\Omega)} & + & a^\varepsilon(\, u^* \circ \widehat{W}^\varepsilon \ , \ v\,) \\ \\ = \ (f,v)_{L^2(\Omega)} & + & \displaystyle\int_{\Gamma^1} \Phi(t)\, v\, d\sigma \ - \ a^\varepsilon(\, \widehat{r}^\varepsilon \ , \ v\,) \end{array} \tag{9}$$

$\forall v \in V$, where the last term tends to zero. Dropping it and choosing an adequate subspace of V should yield a good approximation of (3). From the additional regularity $\widehat{w}^\varepsilon \in W^{1,\infty}(\Omega;\mathbb{R}^n)$, we can define a closed subspace of V

$$V^\varepsilon \;=\; \{v^\varepsilon \in V\,;\, \exists\, v \in V\,,\; v^\varepsilon \;=\; v \circ \widehat{w}^\varepsilon\,\}\,, \tag{10}$$

since $\widehat{w}^\varepsilon \in W^{1,\infty}(\Omega;\mathbb{R}^n)$ implies that $v \circ \widehat{w}^\varepsilon$ belongs to V as soon as v does. We defined the approximate variational formulation as:

find $u \in L^2\,(0,T;V) \cap C^0\left(0,T;L^2(\Omega)\right)$ such that

$$\left\{\begin{array}{l} \dfrac{d}{dt}\left(\rho^\varepsilon(x)\; u \;\circ\; \widehat{W^\varepsilon}, v\right)_{L^2(\Omega)} \;+\; a^\varepsilon(u \;\circ\; \widehat{W^\varepsilon}(t), v) \;=\; (f,v)_{L^2(\Omega)} \;+\; \displaystyle\int_{\Gamma^1} \Phi(t)\, v d\sigma \\ \\ u \;\circ\; \widehat{W^\varepsilon}(0) = u_0 \end{array}\right. \tag{11}$$

for all $v \in V$. By the Lax-Milgram theorem (11) admits a unique solution $u \circ \widehat{W^\varepsilon}$ in $L^2\,(0,T;V^\varepsilon)$. In the following, we will call u *the substituting homogenized solution* and like in [1], we remark that u actually depends on ε but it oscillates less compared to u_ε (see also [11]).

3 Multiscale finite element method and time-stepping method

3.1 Approximation of the oscillating test functions

Recall the local approximation of the oscillating test functions used in [1] for a two-phase composite material simulation. For simplicity we assume $\Omega \subset \mathbb{R}^2$. Our approach can easily be generalized to higher dimensions. We first introduce a coarse mesh of Ω which, for simplicity, is assumed to be polyhedral. This coarse mesh is a conforming triangulation $\mathcal{T}_h$ such that

$$\overline{\Omega} \;=\; \bigcup_{K \in \mathcal{T}_h} K$$

where the elements K satisfy $\mathrm{diam}(K) \leq h$ and the mesh size h is larger than the space scale of oscillations ε, i.e. $h > \varepsilon$.
Then, each oscillating test function $\widehat{w}_i^\varepsilon$ is localy (i.e. in each coarse cell K) approximate by $\widehat{w}_i^{\varepsilon,K}$ solution of

$$\left\{\begin{array}{rcll} -\mathrm{div}\{A^\varepsilon(x)\,\mathrm{grad}\,\widehat{w}_i^{\varepsilon,K}\} & = & 0 & \text{in } K, \\ \widehat{w}_i^{\varepsilon,K} & = & b_i^{\varepsilon,K}(x) & \text{on } \partial K, \end{array}\right. \tag{12}$$

where, on each side S of the cell K, $b_i^{\varepsilon,K}(x)$ is either equal to x_i if $S \cap \partial\Omega \neq \emptyset$ or is the solution of the following boundary value problem. If the side S

is parametrized by a curvilinear coordinate $s \in [0,1]$, the boundary data $b_i^{\varepsilon,K}(x(s))$ is the solution of

$$-\frac{d}{ds}\left(A^\varepsilon(x(s))\frac{d\, b_i^{\varepsilon,K}}{ds}\right) = 0 \quad \text{for } x(s) \in S,$$

with the following boundary conditions at the two end points of S (which are corners of K)

$$b_i^{\varepsilon,K}(x(0)) = x_i(0) \quad b_i^{\varepsilon,K}(x(1)) = x_i(1).$$

These boundary conditions (see [8], [1]) are introduced to allow the necessary oscillating character of the oscillating functions on the coarse cell boundaries. Collecting together these local approximations we define $\widehat{w}_i^{\varepsilon,h} \in H^1(\Omega)$ by $\widehat{w}_i^{\varepsilon,h} = \widehat{w}_i^{\varepsilon,K}$ for each $K \in \mathcal{T}_h$, and we set $\widehat{w}^{\varepsilon,h} = \left(\widehat{w}_1^{\varepsilon,h}, \ldots, \widehat{w}_n^{\varepsilon,h}\right) \in H^1(\Omega;\mathbb{R}^n)$.
A numerical approximation of the local oscillating test functions defined in (12) is computed by using a classical conforming finite element in each $K \in \mathcal{T}_h$ ($\mathbb{P}_{k'}$ Lagrange for example). We use the same notations except that we drop the *hat notation* to refer the approximations. In numerical practice we content ourselves in using $\mathbb{P}_1$ finite elements for computing $w^{\varepsilon,h}$.

3.2 Semi-discretization in space

The use of our multiscale finite element method is straightforward to obtain a semi-discretization of the problem (11).
Let $V_h \subset V$ be a finite dimensional subspace ($\dim V_h = N_h$) corresponding to a conforming finite element method defined on the coarse mesh (12). Typically we use $\mathbb{P}_k$ Lagrange finite elements. Let $\left(\Phi_l^h\right)_{l=1,\ldots,N_h}$ denote a finite element basis of V_h. In order to compute a numerical approximation u_h of the substituting homogenized solution u, we introduce an *oscillating (or multiscale) finite element basis* defined by

$$\Phi_l^{\varepsilon,h}(x) \;=\; \Phi_l^h \circ w^{\varepsilon,h}(x)\;,\;\; (l = 1, ..., N_h). \tag{13}$$

Therefore we obtain a conformal finite element method associated to the coarse mesh $\mathcal{T}_h$ and we denote by $V_h^\varepsilon \subset V$ the space spanned by the functions $\left(\Phi_l^{\varepsilon,h}\right)_{l=1,\ldots,N_h}$. Roughly speaking, V_h^ε is the space "$V_h \circ w^{\varepsilon,h}$".
Denoting $W^{\varepsilon,h} = \left(w_1^{\varepsilon,h}(x), t\right)$, and from the approximate variational formulation (4), we deduce a numerical approximation:
Find $u_h \circ W^{\varepsilon,h} \in V_h^\varepsilon$ such that

$$\frac{d}{dt}\left(\rho^{\varepsilon}(x)\, u_h \circ W^{\varepsilon,h}, v_h \circ\, W^{\varepsilon,h}\right)_{L^2(\Omega)} \quad + \quad a^{\varepsilon}(u_h \circ W^{\varepsilon,h}, v_h \circ W^{\varepsilon,h})$$

$$= \left(f, v_h \circ\, W^{\varepsilon,h}\right)_{L^2(\Omega)} \quad + \quad \int_{\Gamma^1} \Phi(t)\, v_h \circ\, W^{\varepsilon,h} d\sigma \tag{14}$$

for all $v_h \circ W^{\varepsilon,h} \in V_h^{\varepsilon}$ and $u_h \circ W^{\varepsilon,h}(0) = u_0$.

3.3 Time discretization

Checking the approximation of u^{ε} in the form

$$u_h \circ W^{\varepsilon,h}(x,t) \;=\; \sum_{l=1}^{N_h} u_{h,l}(t)\Phi_l^{\varepsilon,h}(x)$$

we are lead to solve the differential system

$$\mathbb{M}^{\varepsilon}\frac{d\{u_h(t)\}}{dt} \;+\; \mathbb{K}^{\varepsilon}\{u_h(t)\}(t) = F^{\varepsilon}(t)$$

where $\mathbb{M}^{\varepsilon}$, $\mathbb{K}^{\varepsilon}$ are respectively the mass and the stiffness matrices and F^{ε} the right hand side coming from the multiscale finite element discretisation. The vector $\{u_h(t)\} \in \mathbb{R}^{N_h}$ represent the approximated values at time t of the substituting homogenized solution at the nodes of the coarse mesh.
Then, we solve the system with an implicit Euler method (for instance). Let Δt be the uniform time step used for time discretization ($\Delta t = T/M$ where M is the number of time steps). The backward Euler's method takes the form

$$(\mathbb{M}^{\varepsilon} \;+\; \Delta t\, \mathbb{K}^{\varepsilon})\left\{u_{(n+1)}\right\} = \Delta t\, F^{\varepsilon}_{(n+1)} \;+\; \mathbb{M}^{\varepsilon}\left\{u_{(n)}\right\}$$

where $\left\{u_{(n)}\right\} \in \mathbb{R}^{N_h}$ denotes the approximation of the solution at the time $n\Delta t$.

4 Numerical experiments

The numerical experiments presented in this section concern two cases of non-periodic homogenization. In the first one, we consider a transmission problem within a heterogeneous composite material and an homogeneous one. The second numerical experiment concerns a diffusion process from a hole inside an heterogeneous composite material.

4.1 Implementation details

Once the coarse mesh of the domain Ω has been built with triangular elements, the implementation of the implicit Euler scheme using our multiscale method in the $\mathbb{P}_2$ case (denoted by $\mathbb{P}_2$-MSFEM) is achieved in two major steps. In the following, we suppose that the right hand side of the partial differential equation, namely f, is a product of a time dependant function by a spatial one.
The first step consists in assembling the mass and the stiffness matrices (which are supposed not to depend on time) as well as the spatial part of the right hand side. Then, in a second step the time-marching is achieved.
Hence, the first step includes the set of computations (which can be done in parallel) of the oscillating functions as well as the elementary contributions (matrices and right hand sides) from each cell of the coarse mesh for the unsteady problem at hand.
The numerical approximations of the oscillating functions itself are performed by using a classical $\mathbb{P}_1$-Lagrange finite element method. To the end of post-processing, they are saved on files.
More precisely, each coarse element K is meshed with triangles and for each element T of this mesh denoted $\mathcal{T}_{h'}^K$, a weighted mean conductivity is computed. It combines values of conductivity of the materials with the volumic fractions in the element $T \in \mathcal{T}_{h'}^K$ (heterogeneous composite mediums are described by piecewise constant properties). Then, the elementary quantities are computed using a two-dimensional centered trapezoidal rule. After assembling these elementary contributions to build the matrix and the right hand side, and after taking into account the boundary conditions on ∂K, the resulting linear system is solved by the Cholesky method.
Once the calculations of the oscillating functions have be done, we can compute the elementary contributions corresponding to each coarse element K. A two-dimensional seven points Gauss rule is used to compute the contributions of each element T of the local fine mesh $\mathcal{T}_{h'}^K$. The same computing procedure is used to evaluate the weighted mean value for the properties of the media used in these numerical integrations.
Then, assembling these elementary contributions leads to build the mass, the stifness matrices and the spatial part of the right hand side which are used in the second step of the time-stepping method.
The matrix $(\mathbb{M}^\varepsilon + \Delta\, t\mathbb{K}^\varepsilon)$ is factorized once for all at the first step and only the right hand side is updated at all time steps.
Thanks to the backup files of the oscillating functions, the numerical approximation of the solution as well as the flux density are given by a post-processing inside each element of the coarse mesh $\mathcal{T}_h$.

4.2 A transmission problem

In this numerical experimentation, the domain Ω is composed of two parts. The upper one consists in a homogeneous material whereas the lower is a heterogeneous one (see fig. 1). The heterogeneous composite material is made up of a pseudo random distribution of 10^4 spherical inclusions in a background matrix. Both phases are isotropic with a high conductivity $A^\varepsilon(x) = 10^2$ in the inclusions and a lower one $A^\varepsilon(x) = 1$ in the matrix and in the upper homogeneous medium.

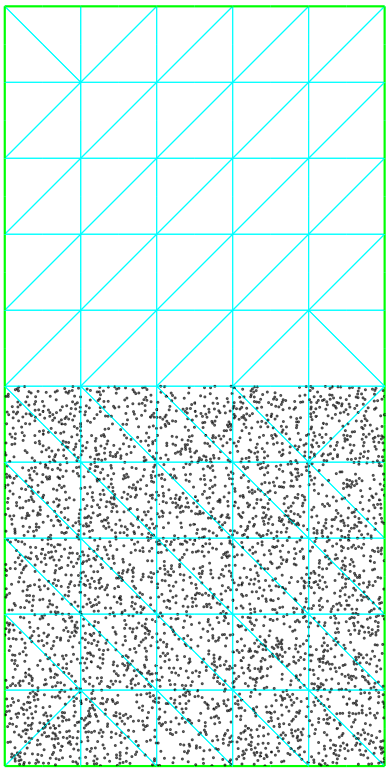

Figure 1: Coarse mesh of the computational domain

This numerical experiment corresponds to a minimum distance between two inclusions of $\varepsilon = 5.10^{-3}$ and a particle diameter of $\varepsilon/2$. A time dependant flux is imposed on the lower part of the boundary of the computational domain. The solution is zero on the upper part of the boundary and satisfies a homogeneous Newman condition on the vertical edges.
At a very small scale, one can clearly see the diffusion channels between close inclusions (see fig. 3).

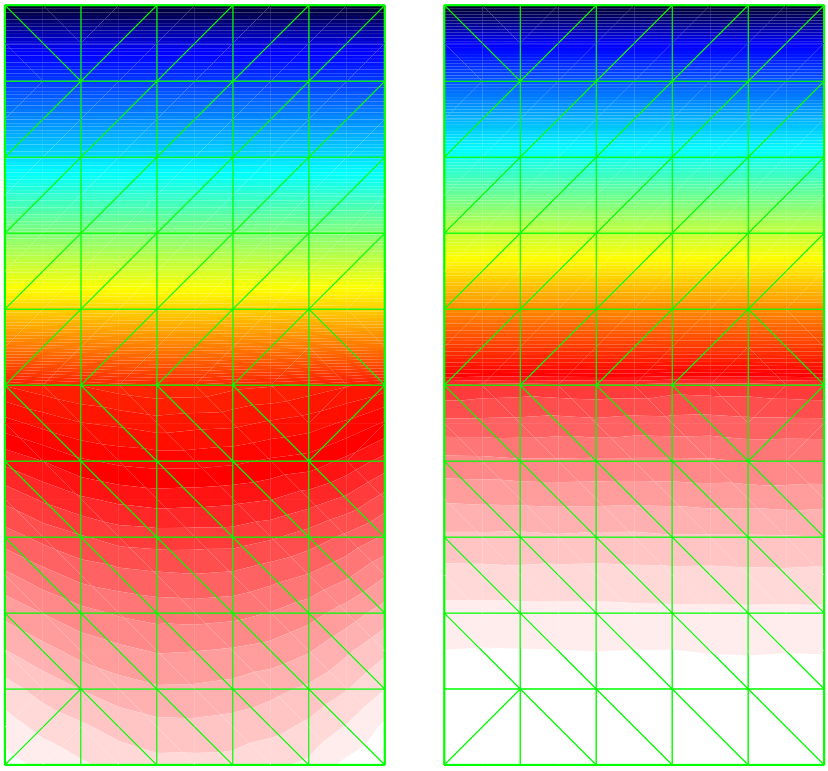

Figure 2: Computed solutions at the 500 and 1000 time step

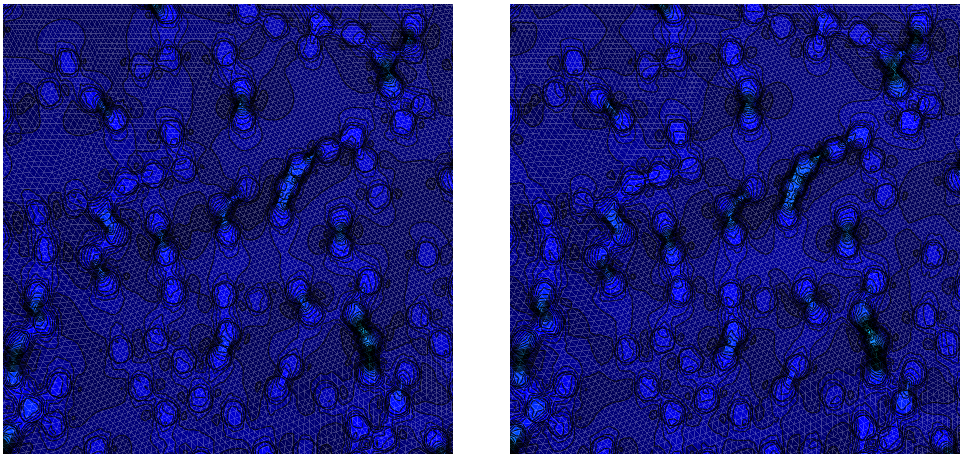

Figure 3: Close-up of the flux density at the 500 and 1000 time step in an element of the coarse mesh.

4.3 A diffusion process from a fissure

From its low permeability and strong capacity for radionucleide retention, the clayey media is a natural geological barrier for nuclear waste storage [3]. Thus, the so-called *Callovo-Oxfordien* geological formation, which is made of *argilite*, was choosen for such a site. In the site of *Bure (France)*, the argilite contains clay (25% to 60%) and other materials such as calcite (15% to 50%), quartz (25% to 30%) pyrite (2% to 3%) and organic material (0.5% to 2%). During the building of repositories, the mechanical excavation of galleries in the clayey rocks leads to damaging their neighbourhoods [4] : many fissures and micro-fissures have been generated. In such a medium, the radionucleide transport is essentially governed by diffusion processes: the dimensionless Peclet number, which gives a rough estimate of the relative signifiance of convective and diffusive transfert, is of order 0.02 for the anions [5].
The aim of the numerical experimentation below is to simulate the diffusion process of radionucleides from a fissure of the excavation disturbed or damaged zone (EDZ) into a region of the clayey media (see fig. 4).

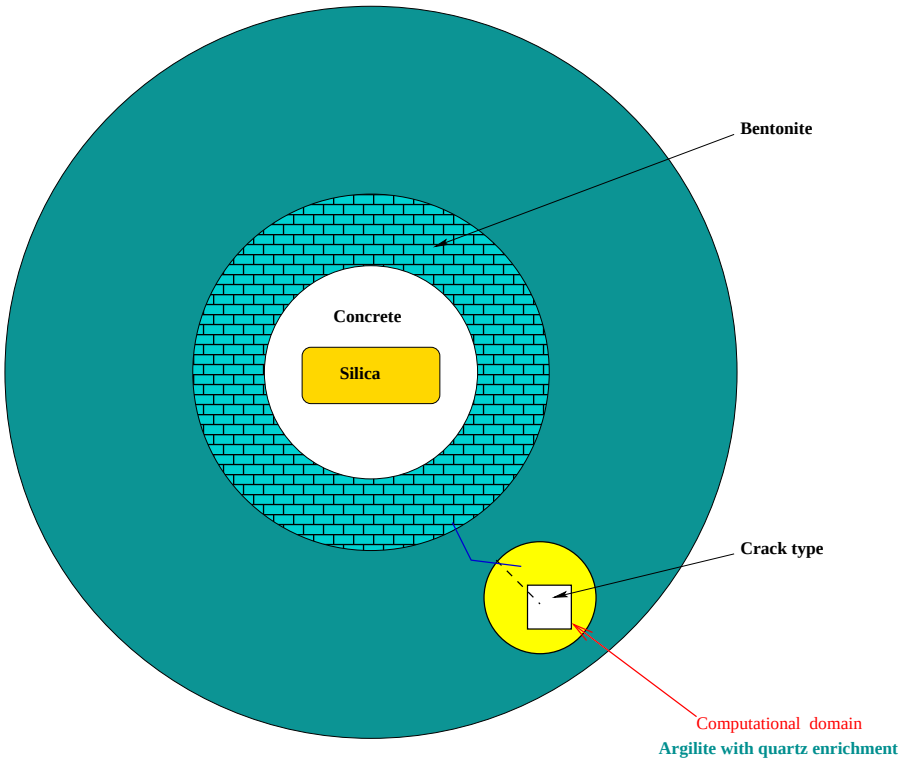

Figure 4: The excavation disturbed or damaged zone (EDZ).

More precisely, we approximate the time-dependant concentration of iodine ^{129}I which is solution of the diffusion equation in a domain Ω (a unit square of one m^2) surrounding the fissure of width $2.0\,10^{-3}m$ (see fig. 5). The diffusion coefficient for ^{129}I in the argilite we have used, is $10^{-10}m^2/s$. Let us note that this one is an effective coefficient and thus it takes into account all the porosity forms inside the medium.

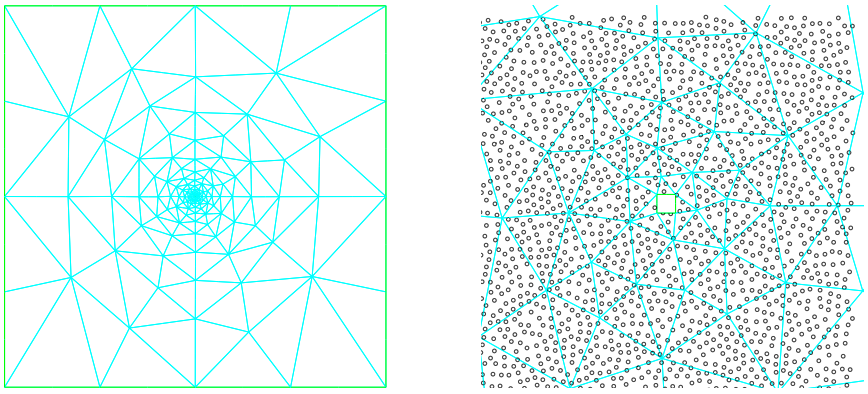

Figure 5: *Coarse mesh of the computational domain and close-up round of the fissure.*

Our simulation assumes that the surrounding fissure contains a quartz enrichment of 12.5% (represented by 10^6 nearly non-diffusive sperical quartz grains of width $0.2\,10^{-3}m$) for which the effective diffusion coefficient is $10^{-28}m^2/year$ ([5]). Note that such an enrichment has been pointed up fifteen kilometers to the North of the storage site ([5]) but is only of 5% to 10% for finest quartz grains.
The diffusing species are supplied from a square shaped source ($2.0\,10^{-3}m$), representing a crack type, centered in the domain Ω. A given flux is given on its boundary Γ^1. The characteristic time scale t_c, related to the characteristic diffusion length L_c, is approximatively $t_c \simeq L_c^2/2. * D_{eff}$ where D_{eff} is the effective diffusion coefficient. Let us note $t_c^{'} = D_{eff}.t_c$. For $L_c = 1/2$, this gives $t_c \simeq 20$ years (ie $t_c^{'} = 0.0625$) and for $L_c = 3/4$, $t_c \simeq 44$ years (ie $t_c^{'} = 0.140625$). The function Φ which describes the time behaviour of the flux density through the hole is one mass unit per $m^{-2}.s^{-1}$ during 20 years and decrease linearly during 24 years. After this period the flux density is zero. The total duration of the numerical integration is 64 years (ie $t_c^{'} = 0.2$). The concentration is supposed to be zero on the exterior boundary Γ^0 of Ω. The time step $\Delta t^{'}$ of the numerical integration is 10^{-3}.
Another simulation of this time evolution has been made without enrichment of quartz : the only material considered here is the argilite (see fig. 7). As expected the enrichment of quartz contributes to a retardation effect of the iodine transport (see fig. 8)). From this simulation and from the previous

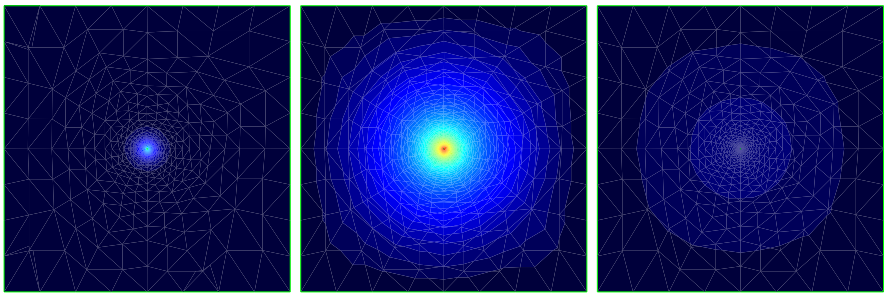

Figure 6: Numerical simulation with a $\mathbb{P}_2$-MSFEM. The figures show the numerical homogenized concentration of iodine ^{129}I at the different time steps (2, 63 and 200).

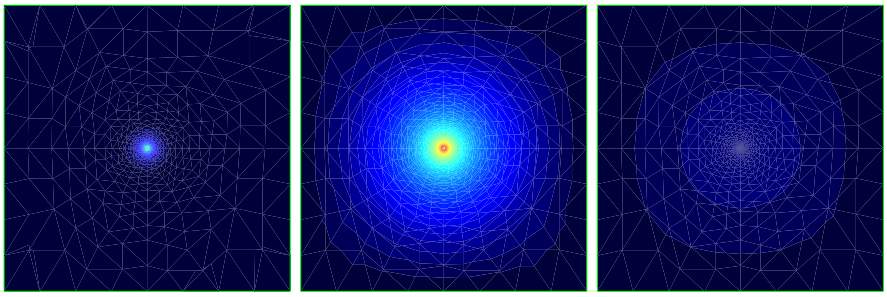

Figure 7: Numerical simulation with a $\mathbb{P}_2$-FEM. The figures show the numerical homogenized concentration of iodine ^{129}I at the same time steps in argilite without enrichment of quartz.

one, we deduce the mean radius of two same valued level lines obtained at the end of the time integration. The square of the ratio of this mean radius gives the factor for an approximation of a new effective diffusion coefficient : the two-phase composite material used for our simulation (which is made up of quartz spherical inclusions in an argilite background matrix) corresponds to a homogeneous one with an effective diffusion coefficient equal to a factor 0.92 of an argilite one.
However, this numerical result must be specified since on the one hand the experimental diffusion coefficients are known with a high uncertainty and on the other hand our model does not take into account that arround the inclusions of quartz grains there exist a porosity filled with water which increase the diffusion (see fig. 9).

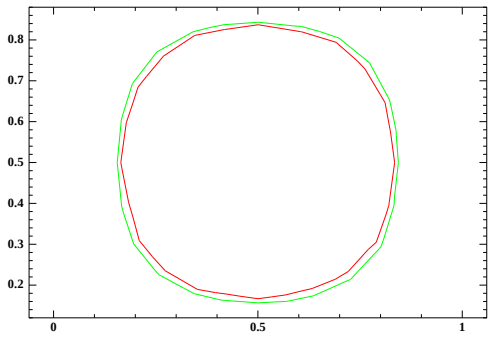

Figure 8: Superposition of two same valued level lines obtained at the end of the time integration. The exterior one corresponds to the homogeneous case (ie without enrichment of quartz).

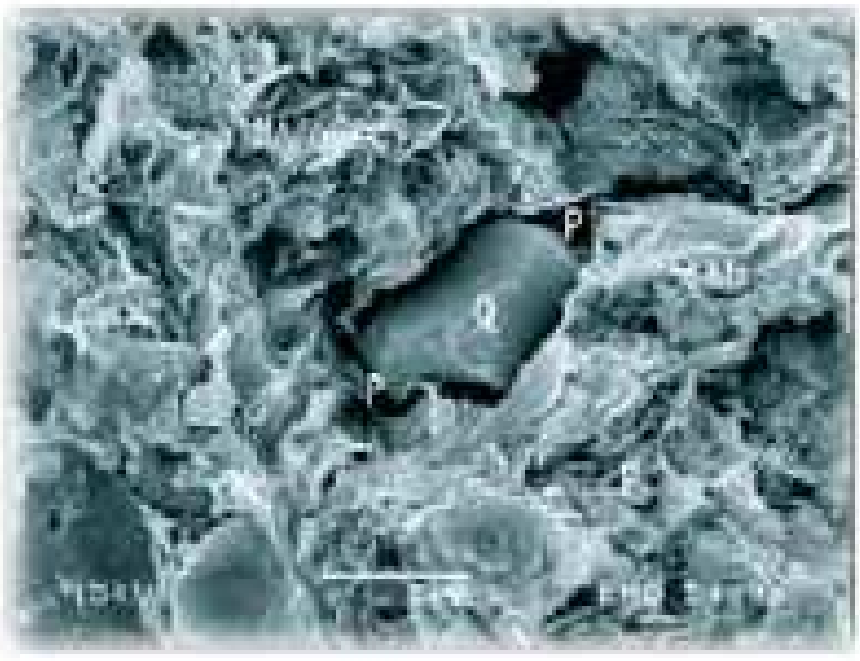

Figure 9: Argilite of so-called *Callovo-Oxfordien* French geological formation: pore (P), quartz (Q) and clay minerals [5].

Acknowledgments

- Both authors' work has been supported by the GdR *MoMaS* (CNRS-2439) sponsored by ANDRA, BRGM, CEA and EDF whose support is gratefully acknowledged .

- Alexandre DIMANOV (LMS-Ecole Polytechnique) is gratefully acknowledged for the many discussions about the nuclear waste storage.

References

[1] G. ALLAIRE, R. BRIZZI, *A multiscale finite element method for numerical homogenization,* SIAM, Multiscale Modeling and Simulation, Vol. 4, No.3 (2005)

[2] G. ALLAIRE, *Shape Optimization by the homogenization method*, Applied Mathematical Sciences, 146, Springer, (2002).

[3] ANDRA, Dossier 2005 Argile, Tome *Synthèse: Evaluation de la faisabilité du stockage géologique en formation argileuse.*, Collection Les Rapports, Décembre 2005.

[4] ANDRA, Dossier 2005 Argile, Tome *Architecture et gestion du stockage géologique*, Collection Les Rapports, Décembre 2005.

[5] ANDRA, Dossier 2005 Argile, Tome *Evolution phénoménologique du stockage géologique*, Collection Les Rapports, Juin 2005.

[6] A. BENSOUSSAN, J.L. LIONS and G. PAPANICOLAOU, *Asymptotic analysis for periodic structures*, Studies in Mathematics and its applications, Vol. 5, North-Holland Publishing company, (1978).

[7] S. BRAHIM-OTSMANE, G. FRANCFORT, F. MURAT, *Correctors for the homogenization of the wave and heat equations*, J. Math. Pures Appl. (9) 71 (1992)

[8] T. Y. HOU, X.-H. WU, *A multiscale finite element method for elliptic problems in composite materials and porous media*, Journal of computational physics 134, 169-189, (1997).

[9] T. Y. HOU, X.-H. WU, Z. CAI, *Convergence of a multiscale finite element method for elliptic problems with rapidly oscillating coefficients*, Math. of Comp. 68, 913-943, (1999).

[10] F. MURAT, L. TARTAR, *H-convergence*, in Topics in the mathematical modeling of composite materials, A. Cherkaev and R.V. Kohn eds., series : Progress in Nonlinear Differential Equations and their Applications, Birkhaüser, Boston 1997. French version : mimeographed notes, séminaire d'Analyse Fonctionnelle et Numérique de l'Université d'Alger (1978).

[11] H. OWHADI and L. ZHANG, *Homogenization of parabolic equations with a continum of space and time scales.*, to appear in Comm. on Pure and Applied Mathematics.